

Effects of Metal Nanoparticles on the Secondary Ion Yields of a Model Alkane Molecule upon Atomic and Polyatomic Projectiles in Secondary Ion Mass Spectrometry

Nimer Wehbe, Andreas Heile, Heinrich F. Arlinghaus, Patrick Bertrand, and Arnaud Delcorte

Anal. Chem., **2008**, 80 (16), 6235-6244 • DOI: 10.1021/ac800568y • Publication Date (Web): 17 July 2008

Downloaded from <http://pubs.acs.org> on November 27, 2008

More About This Article

Additional resources and features associated with this article are available within the HTML version:

- Supporting Information
- Access to high resolution figures
- Links to articles and content related to this article
- Copyright permission to reproduce figures and/or text from this article

[View the Full Text HTML](#)

Effects of Metal Nanoparticles on the Secondary Ion Yields of a Model Alkane Molecule upon Atomic and Polyatomic Projectiles in Secondary Ion Mass Spectrometry

Nimer Wehbe,^{*,†} Andreas Heile,[‡] Heinrich F. Arlinghaus,[‡] Patrick Bertrand,[†] and Arnaud Delcorte[†]

Unité de Physico-Chimie et de Physique des Matériaux, Université Catholique de Louvain, Croix du Sud 1, Louvain-la-Neuve B-1348, Belgium, and Physikalisches Institut, Westfälische Wilhelms-Universität Münster, Wilhelm-Klemm-Str. 10; D-48149 Münster, Germany

A model alkane molecule, triacontane, is used to assess the effects of condensed gold and silver nanoparticles on the molecular ion yields upon atomic (Ga^+ and In^+) and polyatomic (C_{60}^+ and Bi_3^+) ion bombardment in metal-assisted secondary ion mass spectrometry (MetA-SIMS). Molecular films spin-coated on silicon were metallized using a sputter-coater system, in order to deposit controlled quantities of gold and silver on the surface (from 0 to 15 nm equivalent thickness). The effects of gold and silver islets condensed on triacontane are also compared to the situation of thin triacontane overlayers on metallic substrates (gold and silver). The results focus primarily on the measured yields of quasi-molecular ions, such as $(\text{M} - \text{H})^+$ and $(2\text{M} - 2\text{H})^+$, and metal-cationized molecules, such as $(\text{M} + \text{Au})^+$ and $(\text{M} + \text{Ag})^+$, as a function of the quantity of metal on the surface. They confirm the absence of a simple rule to explain the secondary ion yield improvement in MetA-SIMS. The behavior is strongly dependent on the specific projectile/metal couple used for the experiment. Under atomic bombardment (Ga^+ , In^+), the characteristic ion yields an increase with the gold dose up to ~ 6 nm equivalent thickness. The yield enhancement factor between gold-metallized and pristine samples can be as large as ~ 70 (for $(\text{M} - \text{H})^+$ under Ga^+ bombardment; 10 nm of Au). In contrast, with cluster projectiles such as Bi_3^+ and C_{60}^+ , the presence of gold and silver leads to a dramatic molecular ion yield decrease. Cluster projectiles prove to be beneficial for triacontane overlayers spin-coated on silicon or metal substrates (Au, Ag) but not in the situation of MetA-SIMS. The fundamental difference of behavior between atomic and cluster primary ions is tentatively explained by arguments involving the different energy deposition mechanisms of these projectiles. Our results also show that Au and Ag nanoparticles do not induce the same behavior in MetA-SIMS of triacontane. The microstructures of the metallized layers are also different. While metallic sub-

strates provide higher yields than metal islet overlayers in the case of silver, whatever the projectile used, the situation is reversed with gold.

Static time-of-flight secondary ion mass spectrometry (TOF-SIMS) is a powerful method of surface characterization.^{1,2} Benefitting from its ability to study different kinds of solids, this technique has been largely used for many years for the analysis of biological materials,^{3–5} polymers,^{6–9} and metal samples.¹⁰ In addition to its capability to provide molecular information from sample surfaces, TOF-SIMS also proved its high sensitivity for surface imaging.^{11–17} It has been successfully used to record images of the surface distribution of detected elements and molecules with a submicrometer lateral resolution. The diversity of applications involving TOF-SIMS justifies the ceaseless attempts to improve the analytical conditions of the technique. One of the

- (1) Benninghoven, A.; Rüdenauer, F. G.; Werner, H. W. *Secondary Ion Mass Spectrometry, Chemical Analysis*, Vol. 86; J. Wiley: New York, 1987.
- (2) Vickerman, J. C. In *ToF-SIMS: Surface Analysis by Mass Spectrometry*; Vickerman, J. C., Briggs, D., Eds.; Surface Spectra/IMP Publications: Chichester, U.K., 2001; Chapter 1.
- (3) Wagner, M. S.; Castner, D. G. *Langmuir* **2001**, *17* (15), 4649.
- (4) Weibel, D.; Wong, S.; Lockyer, N.; Blenkinsopp, P.; Hill, R.; Vickerman, J. C. *Anal. Chem.* **2003**, *75* (7), 1754–1764.
- (5) McArthur, S. L.; Vendettuoli, M. C.; Ratner, B. D.; Castner, D. G. *Langmuir* **2004**, *20* (9), 3704–3709.
- (6) Cheng, H.; Cornelio Clark, P. A.; Hanton, S. D.; Kung, P. *J. Phys. Chem. A* **2000**, *104* (12), 2641–2647.
- (7) McIntyre, N. S.; Chauvin, W. J.; Martin, R. R. *Anal. Chem.* **1984**, *56* (8), 1519–1521.
- (8) Piwowar, A. M.; Gardella, J. A., Jr. *Anal. Chem.* **2007**, *79* (11), 4126–4134.
- (9) Van Vaeck, L.; Adriaens, A.; Gijbels, A. *Mass Spectrom. Rev.* **1999**, *18*, 1–47.
- (10) Fallavier, M.; Kirsch, R.; Morozov, S. N.; Poizat, J. C.; Thomas, J. P.; Wehbe, N. *Phys. Rev. B* **2003**, *68*, 140102.
- (11) Nygren, H.; Malmberg, P.; Kriegeskotte, C.; Arlinghaus, H. F. *FEBS Lett.* **2004**, *566*, 291–293.
- (12) Chabala, J. M.; Soni, K. K.; Li, J.; Gavrilov, K. L.; Levi-Setti, R. *Int. J. Mass Spectrom. Ion Processes* **1995**, *143*, 191–212.
- (13) Altelaar, A. F. M.; van Minnen, J.; Jimenez, C. R.; Heeren, R. M. A.; Piersma, S. R. *Anal. Chem.* **2005**, *77* (3), 735–741.
- (14) Lockyer, N. P.; Vickerman, J. C. *Appl. Surf. Sci.* **2004**, *231–2*, 377–384.
- (15) Sjøvall, P.; Lausmaa, J.; Johansson, B. *Anal. Chem.* **2004**, *76*, 4271–4278.
- (16) Nygren, H.; Börner, K.; Hagenhoff, B.; Malmberg, P.; Mansson, J. E. *Biochim. Biophys. Acta: Mol. Cell Biol. Lipids* **2005**, *1737*, 102–110.
- (17) Ostrowski, S. G.; Kurczyk, M. E.; Roddy, T. P.; Winograd, N.; Ewing, A. G. *Anal. Chem.* **2007**, *79* (10), 3554–3560.

* Corresponding author. Phone: +32 10 47 85 66. Fax: + 32 10 47 34 52. E-mail: Nimer.wehbe@uclouvain.be.

[†] Université Catholique de Louvain.

[‡] Westfälische Wilhelms-Universität Münster.

major challenges in this research area concerns the development of new methods in order to overcome the low secondary ion yields. Two main routes have been widely explored to reach this goal. The first one is the introduction of polyatomic primary ions, or clusters, which have shown their capability to strongly increase the ion yields compared to those measured under atomic bombardment.^{18–21} This interesting feature encouraged analysts to use polyatomic projectiles such as Au_n^+ , Bi_n^+ , C_{60}^+ , and SF_5^+ for both surface characterization^{4,22–24} and imaging.^{25,26} In addition to the properties of the projectiles, specific sample preparation protocols constitute another solution to improve the molecular ion yields. It has been shown that mixing the sample with specific agents such as molecules and salts can significantly increase the secondary ion yields as well as the sensitivity in chemical imaging.^{27,28} It is believed that the procedure to mix samples with specific agents mainly influences the ionization probability. The use of noble metal substrates instead of conventional substrates also showed a positive effect on the secondary ion yields.²⁹ Understandably, this effect disappears when the layer to be analyzed becomes thick with respect to the sampling depth of SIMS. Finally, the evaporation of a small quantity of noble metal such as Au and Ag on top of the sample surface constitutes a third approach. This method is easy and can be readily applied to any kind of sample. Noble metal evaporation on top of organic samples, associated with SIMS analysis (MetA-SIMS), has been successfully used for ion signal enhancement with different kinds of materials such as polymers^{30–35} and organic molecules^{35–38} and for improvement of surface imaging.^{39–41} Nevertheless the effect of the metal evaporation on the ion yields is strongly dependent

on the choice of projectile. In a first series of studies, the usefulness of this technique was demonstrated in the case of atomic projectiles, with molecular ion yield enhancement sometimes larger than 2 orders of magnitude.^{37,38,40} In turn, it was hoped that combining metallization with polyatomic projectiles might lead to even larger yields than using polyatomic projectiles alone. However preliminary results obtained with polyatomic projectiles are not convincing. In some cases, the signal slightly increases³⁶ while, in most cases, metallization combined with polyatomic projectiles has a negative effect on the useful ion yields.^{42–44}

This paper presents a systematic study undertaken with one molecule (triacontane) used as a model in order to assess the effect of gold and silver evaporation on the secondary ion yields for a range of primary projectiles. The results and discussions will be focused on the quasi-molecular ions such as $(\text{M} - \text{H})^+$ and $(2\text{M} - 2\text{H})^+$ and on the metal-cationized molecular ions such as $(\text{M} + \text{Au})^+$, $(\text{M} + \text{Ag})^+$. A comparison will be finally made between gold and silver evaporation on top of triacontane samples and spin-coating of the same molecule on gold and silver substrates. For this study, we used four different projectiles, both atomic (Ga^+ and In^+) and polyatomic (C_{60}^+ and Bi_3^+). The results confirm the absence of a unique rule to explain the secondary ion yield improvement in MetA-SIMS. They are tentatively interpreted on the basis of empirical and theoretical arguments.

MATERIALS AND METHODS

Sample. The triacontane molecule ($\text{C}_{30}\text{H}_{62}$, formula weight ~ 422.5) was purchased from Aldrich Chemie in the form of crystal powder. The crystal powder was first dissolved in benzene to a concentration of ~ 10 mg/mL. This solution was subsequently spin-coated on a clean silicon wafer, and the samples were metallized afterward, by evaporating various quantities of gold and silver on the surface. With this procedure, pristine molecular samples and samples metallized with increasing metal deposit (from 0 up to 15 nm equivalent thickness) were obtained. The third set of samples was prepared by evaporating 40 nm of metal directly onto the silicon wafer in order to obtain gold and silver substrates; the solution of triacontane was subsequently spin-coated on these metal substrates. Spincoating was performed using a KARL SUSS spin coater, by letting a droplet of the sample solution evaporate at 5000 rpm during 60 s. Metal deposition was carried out using a Cressington 208HR sputter coater system. The deposited metal amount was measured using a quartz crystal microbalance with a resolution of about 0.1 nm (equivalent thickness). Prior to organic sample spincoating and/or gold–silver metallization, the silicon substrates were rinsed in 2-propanol and hexane and dried in a stream of hot air.

The scanning electron microscopy (SEM) images were recorded using a Zeiss Leo 982 apparatus (5 keV primary electron beam energy).

- (18) Kollmer, F. *Appl. Surf. Sci.* **2004**, *231–232*, 153–158.
- (19) Sigmund, P. In *Sputtering by Particle Bombardment I*; Behrisch, R., Ed.; Topics in Applied Physics, Vol. 47; Springer: New York, 1981.
- (20) Sigmund, P. *Phys. Rev.* **1969**, *184*, 383. Sigmund, P. *Phys. Rev.* **1969**, *187*, 768.
- (21) Sigmund, P.; Claussen, C. J. *Appl. Phys.* **1981**, *52*, 990.
- (22) Gillen, G.; Roberson, S. *Rapid Commun. Mass Spectrom.* **1998**, *12*, 1303–1312.
- (23) Weibel, D. E.; Lockyer, N.; Vickerman, J. C. *Appl. Surf. Sci.* **2004**, *231–232*, 146.
- (24) Nagy, G.; Gelb, L. D.; Walker, A. V. *J. Am. Soc. Mass Spectrom.* **2005**, *16*, 733.
- (25) Hagenhoff, B.; Pfitzer, K.; Tallarek, E.; Kock, R.; Kersting, R. *Appl. Surf. Sci.* **2004**, *231–232*, 196–200.
- (26) Belu, A. M.; Davies, M. C.; Newton, J. M.; Patel, N. *Anal. Chem.* **2000**, *72*, 5625–5638.
- (27) Locklear, J. E.; Guillemier, C.; Verkhoturov, S. V.; Schweikert, E. A. *Appl. Surf. Sci.* **2006**, *252*, 6624–6627.
- (28) Luxembourg, S. L.; McDonnell, L. A.; Duursma, M. C.; Guo, X.; Heeren, R. M. A. *Anal. Chem.* **2003**, *75*, 2333–2341.
- (29) Bletsos, I. V.; Hercules, D. M.; van Leyen, D.; Hagenhoff, B.; Niehuis, E.; Benninghoven, A. *Anal. Chem.* **1991**, *63*, 1953–1960.
- (30) Delcorte, A.; Bour, J.; Aubriet, F.; Muller, J.-F.; Bertrand, P. *Anal. Chem.* **2003**, *75*, 6875–6885.
- (31) Marcus, A.; Winograd, N. *Anal. Chem.* **2006**, *78*, 141–148.
- (32) Ruch, D.; Boes, C.; Zimmer, R.; Muller, J.-F.; Migeon, H.-N. *Appl. Surf. Sci.* **2003**, *203–204*, 566–570.
- (33) Inoue, M.; Murase, A. *Appl. Surf. Sci.* **2004**, *231–232*, 296–301.
- (34) Inoue, M.; Murase, A.; Segiura, M. *Jpn. Soc. Anal. Chem.* **2004**, *20*, 1623–1628.
- (35) Delcorte, A.; Médard, N.; Bertrand, P. *Anal. Chem.* **2002**, *74*, 4955–4968.
- (36) McDonnell, L. A.; Heeren, R. M. A.; de Lange, R. P. J.; Fletcher, I. W. *J. Am. Soc. Mass Spectrom.* **2006**, *17*, 1195–1202.
- (37) Keune, K.; Boon, J. J. *Surf. Interface Anal.* **2004**, *36*, 1620–1628.
- (38) Adriaensen, L.; Vangaever, F.; Gijbels, R. *Anal. Chem.* **2004**, *76*, 6777–6785.
- (39) Nygren, H.; Malmberg, P. J. *Microscopy* **2004**, *215*, 156–161.
- (40) Altelaar, A. F.; Klinkert, I.; Jalink, K.; de Lange, R. P. J.; Adan, R. A. H.; Heeren, R. M. A.; Piersma, S. R. *Anal. Chem.* **2006**, *78*, 734–742.

- (41) Delcorte, A.; Bertrand, P. *Appl. Surf. Sci.* **2004**, *231–232*, 250–255.
- (42) Delcorte, A.; Yunus, S.; Wehbe, N.; Nieuwjaer, N.; Poleunis, C.; Felten, A.; Houssiau, L.; Pireaux, J.-J.; Bertrand, P. *Anal. Chem.* **2007**, *79*, 3673–3689.
- (43) Wehbe, N.; Delcorte, A.; Heile, A.; Arlinghaus, H. F.; Bertrand, P. *Appl. Surf. Sci.*, In press; DOI 10.1016/j.apsusc.2008.05.068.
- (44) Heile, A.; Lipinsky, D.; Wehbe, N.; Delcorte, A.; Bertrand, P.; Felten, A.; Houssiau, L.; Pireaux, J.-J.; De Mondt, R.; Van Royen, P.; Van Vaeck, L.; Arlinghaus, H. F. *Surf. Interface Anal.* **2008**, *40*, 538–542.

Secondary Ion Mass Spectrometry. The secondary ion mass analyses were performed using four different projectile sources belonging to two different time-of-flight SIMS instruments. The first one was a PHI-EVANS time-of-flight SIMS (TRIFT 1) allowing us to have 15 keV Ga^+ , In^+ , and C_{60}^+ beams. The $^{69}\text{Ga}^+$ beam was obtained from a FEI 83-2 liquid metal ion source (~ 1 nA dc current; 5 kHz frequency; 22 ns pulse width bunched down to 1 ns). In the case of the indium ion beam, $^{115}\text{In}^+$, the dc current was ~ 600 pA and the pulse width ~ 10 ns. The C_{60}^+ measurements were conducted using a primary ion beam system (IOG-C60-20) from Ionoptika Ltd. (~ 160 pA dc current and ~ 20 ns pulse width). To maximize the measured intensities, the secondary ions were postaccelerated by a high voltage (7 kV) in front of the detector. This postacceleration increases the detection efficiency of the emitted ions reaching the front of the microchannel plate detector (MCP).⁴⁵ The TOF-SIMS mass spectra were obtained by collecting the secondary ion signal in the mass range $0 < m/z < 5000$ for the 180 s bombardment of a $120 \times 120 \mu\text{m}^2$ sample area. The experimental setup has been described in detail elsewhere.⁴⁶ The second instrument was a TOF-SIMS instrument equipped with a 25 kV liquid metal ion gun (Bi_m^+ , IONTOF GmbH). In this latter case the mass range for the secondary ion collecting signal was $0 < m/z < 3400$ for the 300 s bombardment of a $150 \times 150 \mu\text{m}^2$ with a dc current of about 0.02 pA. The impact energy of all these projectiles (Ga^+ , In^+ , C_{60}^+ , and Bi_3^+) was 12 keV, and their angle of incidence was 45° . This choice of parameters corresponds to a projectile fluence close to 2×10^{11} ions/ cm^2 for all used primary ion species, ensuring static bombardment conditions.

RESULTS AND DISCUSSION

The major objective of this study is to assess the advantages and drawbacks of noble metal deposition (Au and Ag) in static TOF-SIMS, for a model molecular layer (triacontane) and for two categories of projectiles: atomic ions (Ga^+ and In^+) and cluster (C_{60}^+ and Bi_3^+) ions. In the first part of the results (Projectile Effect on Gold Metallized Triacontane), we investigate the combined effects of different projectiles and gold metallization, first, qualitatively (mass spectra) and, then, in terms of secondary ion yields for selected secondary ions (molecular ions, quasi-molecular ions, Au-cationized molecules, etc). The comparison between the effects observed for gold and silver metallized triacontane samples and for triacontane directly spin-coated on gold and silver substrates will be presented in the second part (Substrate Effect on the Secondary Ion Yields).

Projectile Effect on Gold Metallized Triacontane. Mass Spectra. The six positive secondary ion mass spectra of Figure 1 represent the experimental results obtained when the pristine triacontane sample and two Au-metallized samples (2–10 nm) were bombarded by atomic Ga^+ ions and by Bi_3^+ clusters. The three spectra for Ga^+ bombardment are directly comparable since they have the same scale. However upon Bi_3^+ bombardment, the vertical scales for both Au-metallized samples were multiplied by a factor of 10 for a better visualization of the peaks. The inset spectra show peaks assigned to Au-cationized molecular ions. For Ga^+ bombardment, the intensity of the quasi-molecular ion peaks

increases strongly upon Au metallization, in comparison with the pristine sample. The behavior is completely different upon Bi_3^+ bombardment, since the $(\text{M} - \text{H})^+$ intensity decreases strongly after Au evaporation compared to the pristine sample. Moreover the evaporation of Au on top of these samples allows us to detect the Au-cationized molecular ions, $(\text{M} + \text{Au} - x\text{H})^+$ (inset spectra), with an intensity increasing with the thickness of the gold layer for both projectiles. In addition to the secondary ions shown in Figure 1, other ions of interest were also detected upon Au metallization, among which one can mention $(\text{M} + \text{N} - x\text{H})^+$, $(\text{M} + \text{O} - x\text{H})^+$, $(\text{M} + 2\text{Au} - x\text{H})^+$, $(\text{M} + 3\text{Au})^+$, $(2\text{M} + \text{Au} - x\text{H})^+$, $(2\text{M} + 2\text{Au} - x\text{H})^+$, $(2\text{M} + 3\text{Au} - 2\text{H})^+$ and $(3\text{M} + \text{Au} - x\text{H})^+$. These ions have also been observed in the secondary ion mass spectra of triacontane cast on a gold substrate.⁴⁷ The yield variation of the most characteristic secondary ions as a function of the gold equivalent thickness is analyzed in detail hereafter.

Yields of Quasi-Molecular Ions. In order to establish the best conditions for signal improvement in Meta-SIMS, we monitored the variations of secondary molecular ion yields as a function of the evaporated gold thickness from 0 to 15 nm. These comparisons are displayed in Figure 2 for $(\text{M} - \text{H})^+$, M^+ , $(\text{M} + \text{N} - \text{H})^+$ and $(2\text{M} - 2\text{H})^+$ emitted upon different projectile bombardment. For all these experimental points, the error bars are less than 10%. Once again the evolutions of the secondary ions yields with gold thickness are very dependent on the projectile (atomic or polyatomic). In the case of atomic bombardment (Ga^+ , In^+) one observes a common behavior. All the considered secondary ion yields increase with the thickness of the gold layer up to ~ 6 nm of gold, beyond which they remain almost constant in the investigated metallization range ($\sim 4 \times 10^{-4}$ and $\sim 3 \times 10^{-4}$ for Ga^+ and In^+ , respectively). The yield enhancement factors are reported in Table 1. They are calculated, for each ion, by dividing the maximum secondary ion yield by the yield obtained for the pristine sample. Comparable enhancement factors have been measured, upon Ga^+ bombardment, after evaporation of gold onto Irganox and PVB samples, with respect to untreated samples (enhancement factors = 33 and 50, respectively).^{41,48} We point out that, whatever the projectile, the $(\text{M} - \text{H})^+$ yields are always higher than the $(\text{M})^+$ yields. The formation of positive quasi-molecular ions by hydrogen loss is a common behavior for saturated hydrocarbon molecules in SIMS, while the formation of fully saturated, odd-electron parent ions is not favored.

The evolutions of the quasi-molecular ion yields obtained under polyatomic projectiles bombardment (Bi_3^+ , C_{60}^+) are extremely different than those shown before for atomic projectiles. First, the molecular ion yields, obtained with polyatomic bismuth and fullerene projectiles on pristine samples, are much higher than the yields obtained with atomic indium and gallium primary ions. The highest yields on the pristine sample are obtained with Bi_3^+ followed by C_{60}^+ clusters. For example, upon Bi_3^+ bombardment, the yields of the molecular $(\text{M} - \text{H})^+$ and dimer $(2\text{M} - 2\text{H})^+$ ions are, respectively, 2 and 3 orders of magnitude higher than those obtained with atomic Ga^+ primary ions. However, for both cluster projectiles, the secondary ion yields decrease dramatically with the presence of gold. The drastic yield decrease, which

(45) Gilmore, I. S.; Seah, M. P. *Int. J. Mass Spectrom.* **2000**, *202*, 217–229.

(46) Delcorte, A.; Vanden Eynde, X.; Bertrand, P.; Reich, D. F. *Int. J. Mass Spectrom.* **1999**, *189*, 133.

(47) Delcorte, A.; Bertrand, P. *Surf. Sci.* **1998**, *412/413*, 97–124.

(48) De Mondt, R.; Adriaenssens, L.; Vangaveer, F.; Lenaerts, J.; Van Vaeck, L.; Gijbels, R. *Appl. Surf. Sci.* **2006**, *252*, 6652–6655.

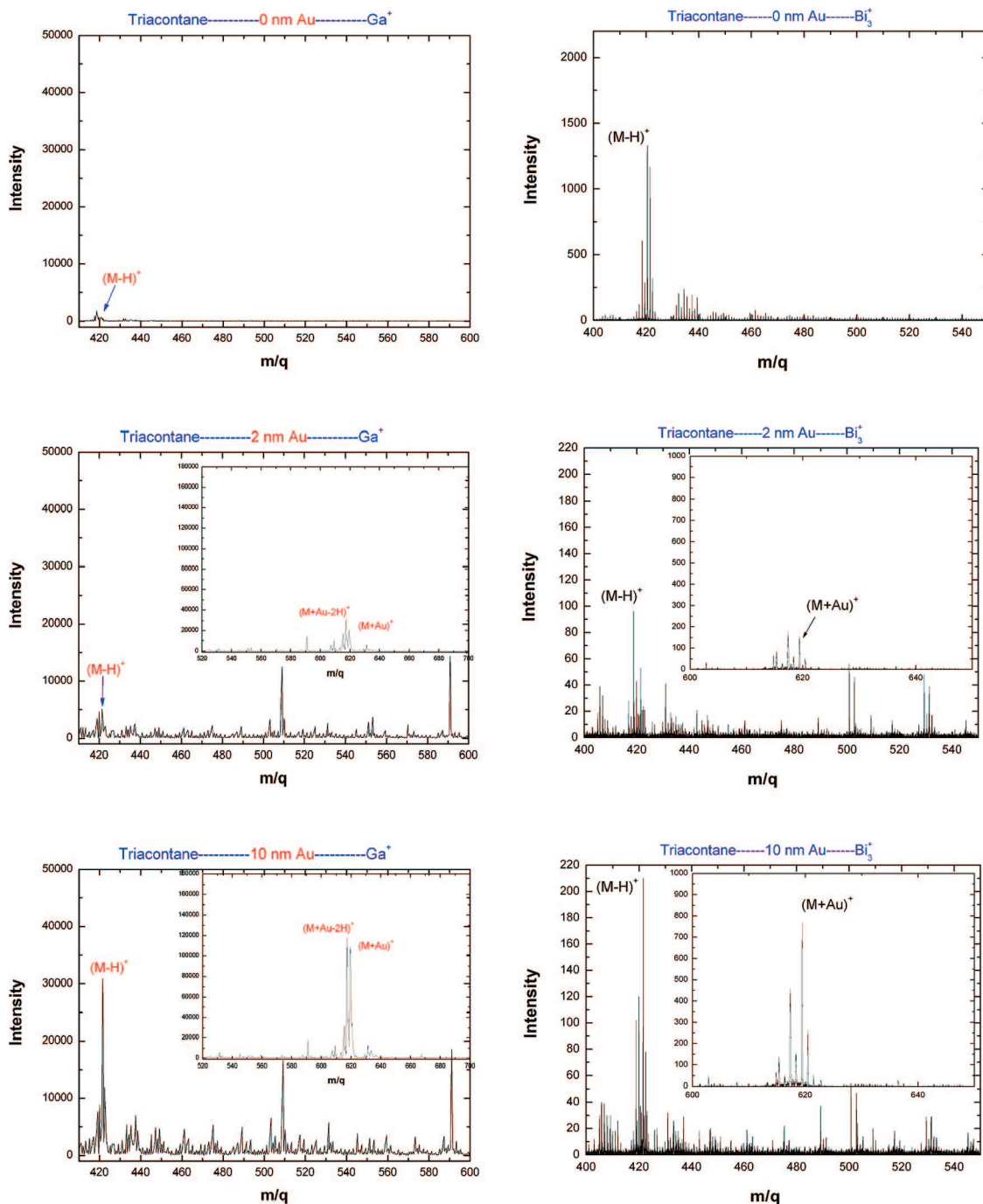


Figure 1. Positive TOF-SIMS spectra of triacontane spin-coated on a Si wafer and analyzed with Ga^+ and Bi_3^+ before metallization (pristine) and after metallization with 2 and 10 nm Au. The inset spectra show peaks assigned to Au-cationized molecular ions.

already occurs for small quantities of gold (0.5 nm), is followed by a slight increase for larger gold doses. A plateau is reached for 4 nm of gold. After the evaporation of 10 nm of gold, the $(\text{M} - \text{H})^+$ yield measured upon Bi_3^+ bombardment is $\sim 2\text{--}3$ times lower than that obtained under In^+ and Ga^+ bombardment. Such a behavior for which the condensation of a gold layer on the surface induces a yield decrease upon polyatomic (SF_5^+ , C_{60}^+ , and Bi_3^+) projectile bombardment has been reported for a series of organic samples (polymers, dyes, peptides).^{42,44}

Yields of Gold-Cationized Ions. Gold-cationized molecular ions $(\text{M} + x\text{Au} - y\text{H})^+$ can be considered as molecular fingerprints for the Au-metallized samples. Figure 3 displays the evolutions of several Au-cationized ions emitted under atomic and polyatomic

projectile bombardment, as a function of the deposited gold quantity. For atomic ions, these results show clearly the usefulness of Au metallization to improve sensitivity in SIMS analysis. First, taking the same quantity of Au evaporated on pristine samples, the yields are always higher for the gold-cationized ions $(\text{M} + \text{Au})^+$ and $(\text{M} + \text{Au} - 2\text{H})^+$ than those measured for the quasi-molecular ions shown in Figure 2. For Ga^+ bombardment, the emission yield of $(\text{M} + \text{Au})^+$ is ~ 13 times larger than the yield of M^+ (for 6 nm of gold).

For the Au metallized samples, the evolutions with Au thickness for the considered Au-cationized ion yields are very similar to those of the quasi-molecular ions (Figure 2) under both atomic and polyatomic projectiles. Indeed, upon Ga^+ and In^+ bombard-

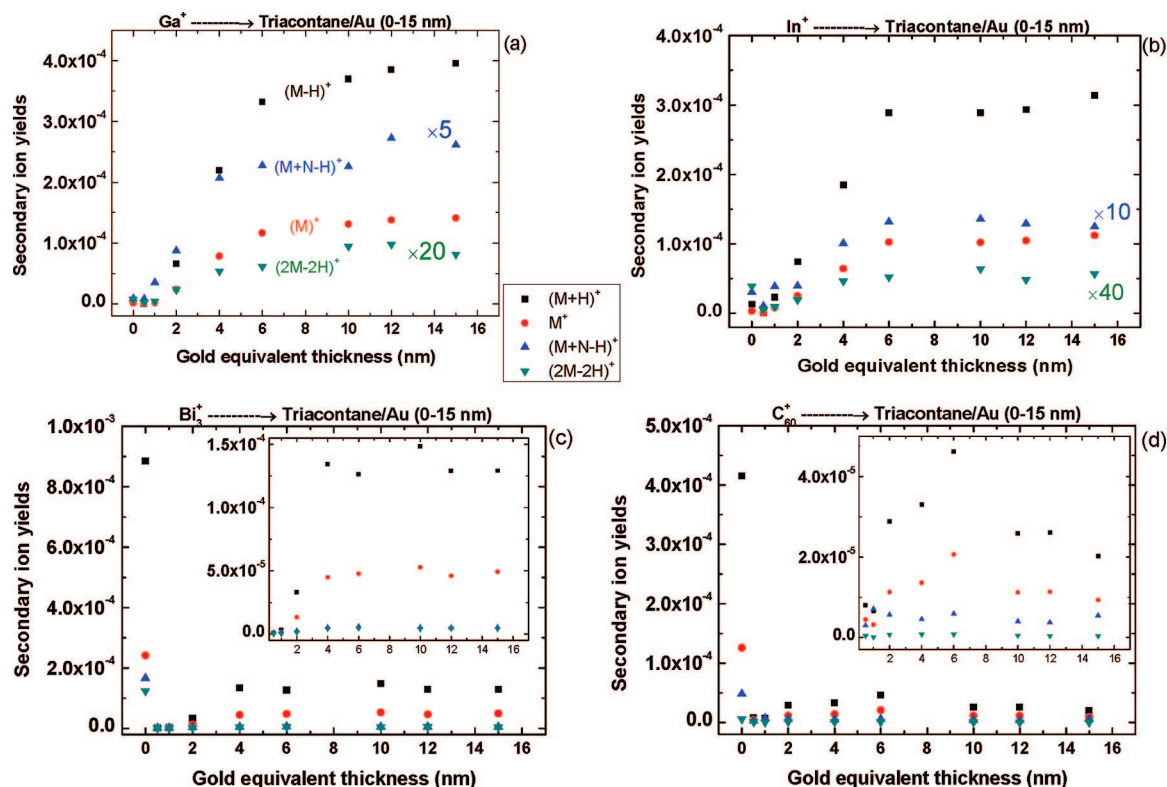


Figure 2. Secondary quasi-molecular ion yields evolutions as a function of the evaporated gold thickness (from 0 to 15 nm) measured upon atomic projectiles Ga⁺/In⁺ (a and b) and upon polyatomic projectiles Bi₃⁺/C₆₀⁺ (c and d). Some curves have been multiplied by different factors for a better visualization of the evolutions.

Table 1. Quasi-Molecular Ion Yields for Triacontane Spin-Coated on Si Wafer Measured for Pristine Sample and after Evaporation of 10 nm Au upon Atomic Projectiles Ga⁺ and In⁺^a

	Ga ⁺ pristine (a)	Ga ⁺ 10 nm Au (b)	enhancement factor-Ga ⁺ (b/a)	In ⁺ pristine (c)	In ⁺ 10 nm Au (d)	enhancement factor-In ⁺ (d/c)
(M - H) ⁺	5.24 × 10 ⁻⁶	3.7 × 10 ⁻⁴	71	1.32 × 10 ⁻⁵	2.93 × 10 ⁻⁴	22
M ⁺	1.56 × 10 ⁻⁶	1.3 × 10 ⁻⁴	83	3.2 × 10 ⁻⁶	1.02 × 10 ⁻⁴	32
(2M - 2H) ⁺	3.75 × 10 ⁻⁷	4.7 × 10 ⁻⁶	13	9.75 × 10 ⁻⁷	1.6 × 10 ⁻⁶	1.64

^a The enhancement factors are calculated, for each ion, by dividing the maximum secondary ion yield by the yield obtained for the pristine sample.

ment (parts a and b of Figure 3, respectively), the yields increase from 0.5 nm of Au up to ~6 nm of Au, beyond which they remain almost constant. The curves obtained with polyatomic projectiles show that bismuth clusters (Figure 3c) provide yields that are, overall, 1 order of magnitude higher than those obtained for fullerenes (Figure 3d). The shape of the yield curves is also different for Bi₃⁺ and C₆₀⁺. In the case of Bi₃⁺, the yields increase from 0.5 nm up to 4 nm of Au, a value beyond which they remain almost constant. For C₆₀⁺, the yields increase from 0.5 nm up to ~4 nm of Au and then they tend to decrease. These yields are also significantly lower than those measured in the case of atomic bombardment (Figure 3). Moreover, the gold thickness needed to reach the maximum yields depends on the projectile type (~6–10 nm for atomic projectiles and ~4 nm for polyatomic projectiles). In the next subsection, the case of pure gold clusters, Au_n⁺, sputtered from the hybrid metal organic surface is investigated.

Yields of Gold Atomic and Cluster Ions. For samples metallized with different Au fluences, Figure 4 presents the evolutions of the emitted atomic ion Au₁⁺ and of the gold clusters Au_n⁺ (*n* =

3, 7, and 13) upon bombardment by Ga⁺, In⁺, Bi₃⁺, and C₆₀⁺. The behavior of these ions, a sustained increase followed by a plateau at large gold coverage, is similar for the two atomic projectiles. For all the projectiles, the secondary ion yields decrease with increasing cluster size (from Au₁⁺ to Au₁₃⁺). Similar observations are also documented in the literature for clusters sputtered from pure metal crystals. Upon Bi₃⁺ bombardment, the yields vary only slightly over the entire range of gold thicknesses. Only the heaviest emitted ion, Au₁₃⁺, displays a monotonic yield decrease from 0.5 until 15 nm of Au. Such an intensity decrease with increasing metal thickness is even clearer upon C₆₀⁺ bombardment. For instance, the Au₃⁺ intensity already shows a significant decay with increasing gold thickness. The yield decrease is more pronounced in the case of Au₇⁺ and Au₁₃⁺.

Looking at the yield values, one must consider two different cases, the atomic ion Au₁⁺ and clusters Au_n⁺ (*n* = 3, 7, and 13) cases. For Au₁⁺, the yields are generally higher when atomic primary ions (Ga⁺, In⁺) are used as projectiles instead of polyatomic (Bi₃⁺, C₆₀⁺). In contrast, gold cluster emission is always favored under polyatomic projectile bombardment. For a

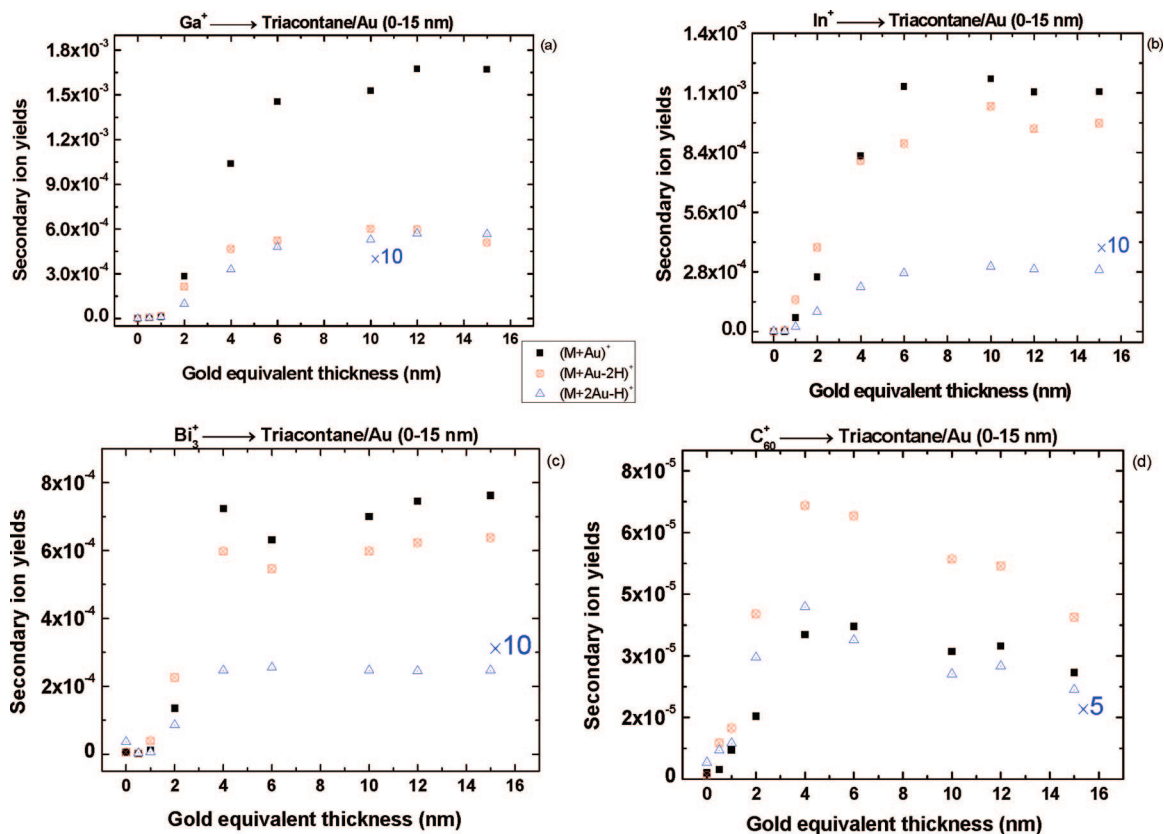


Figure 3. Secondary Au-cationized ion yields evolutions as a function of the evaporated gold thickness (from 0 to 15 nm) measured upon atomic projectiles Ga⁺/In⁺ (a and b) and upon polyatomic projectiles Bi₃⁺/C₆₀⁺ (c and d). The (M + 2Au - H)⁺ curves have been multiplied by factors of 5 or 10 for a better visualization of the evolutions.

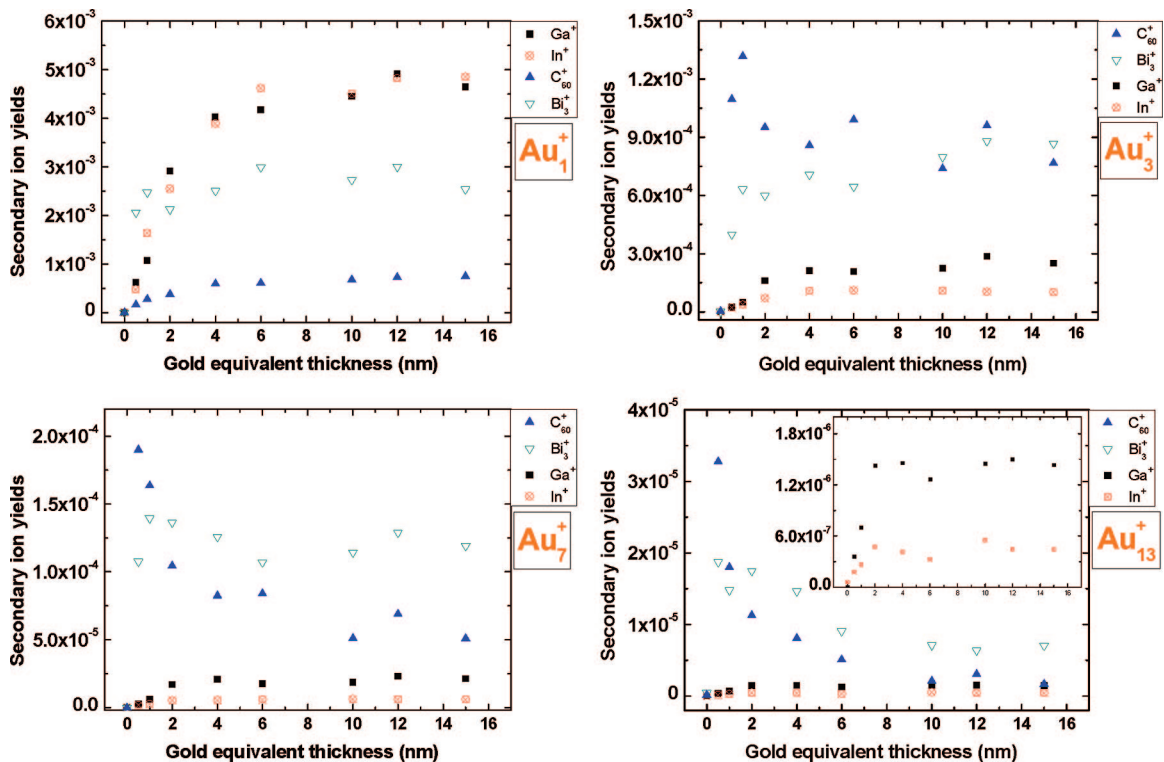


Figure 4. Evolution of the emitted atomic Au₁⁺ as well as gold clusters Au_n⁺ (n = 3, 7, and 13) yields measured under atomic and polyatomic projectiles as a function of the gold equivalent thickness (from 0 to 15 nm).

low amount of evaporated Au (0.5–1 nm), the yields of Au₃⁺–Au₁₃⁺ obtained upon fullerene impact can be 2 orders of

magnitude higher than those measured upon Ga⁺ and In⁺ bombardment. Between Bi₃⁺ and C₆₀⁺, the latter projectile

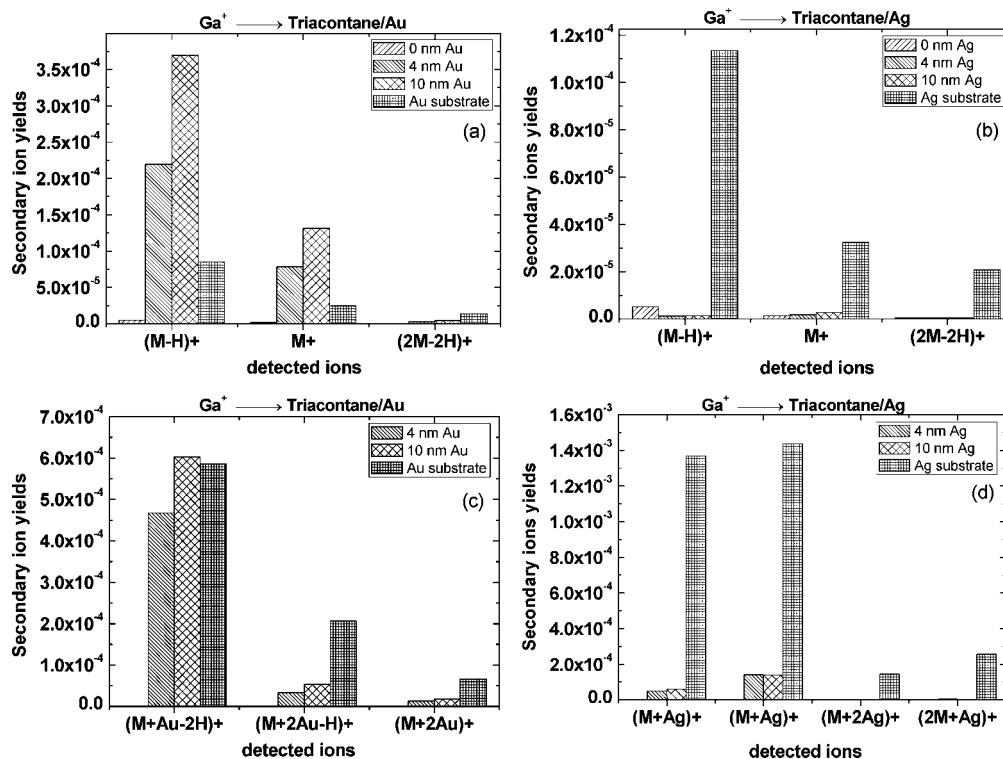


Figure 5. Secondary ion yields measured after gold (a and c) and silver (b and d) evaporation on triacontane layers and, on the other hand, the triacontane spin-coated on gold and silver substrates. In each frame, the yields obtained for pristine sample (for molecular ions) as well as for two different Au/Ag thickness layers (4 and 10 nm) are depicted and compared with the results measured on metal substrate. This comparison is made for several quasi-molecular ions as well as for metal-cationized ions under Ga^+ bombardment.

provides higher yields for Au_3^+ but not for the heavier emitted ions (Au_7^+ and Au_{13}^+). The fact that Au_1^+ ions are emitted with higher yields with atomic projectiles is not unique to this study. Fallavier et al. have shown experimentally that Au_1^- ions emitted from a gold foil under gold projectiles (Au_p^+ , $1 \leq p \leq 9$) show a reduction of the emission yield per incident atom whereas the yields of the emitted gold clusters Au_n^- ($n > 1$) increase with the size p of the incident cluster projectiles.¹⁰ This experimental result is supported by molecular dynamics simulations, which show that, for silicon samples sputtered by Au and Au_2 projectiles, the Si monomer sputtering yield exhibits a linear dependence on projectile size while it is strongly nonlinear in the case of Si emitted clusters.⁴⁹

In the following section, the effects of gold and silver condensates on triacontane will be compared to the situation of thin triacontane layers cast on metallic substrates.

Substrate Effect on the Secondary Ion Yields. *Gold and Silver Metallized Samples upon Ga^+ Bombardment.* The comparison between the secondary ion yields obtained after gold and silver evaporation on triacontane samples and, on the other hand, the triacontane spin-coated on gold and silver substrates is presented in Figure 5. In each frame the molecular ion yields obtained for the pristine sample and for two different Au (Ag) thicknesses (4 and 10 nm) are compared with the results measured for monolayers spin-cast on metal substrates. This comparison is made for several quasi-molecular and metal-cationized ions for Au and Ag metallization. The choice of the metal plays a major role for the yields enhancement of the emitted ions. In the case of gold, several

ions are emitted with higher yields if the triacontane is metallized rather than spin-coated on metal (spin-coating on Au substrate induces yields about 5 times lower for $(\text{M} - \text{H})^+$ and M^+ , Figure 5a). However, the dimer ion $(2\text{M} - 2\text{H})^+$ shows a slightly higher yield for triacontane spin-coated on Au substrate. For silver, spin-coating the triacontane on metal always provides much higher yields than metal evaporation (Figure 5b,d). The yield ratios between metal substrates and metal condensates can reach, for example, the value of 60 for $(2\text{M} - 2\text{H})^+$. One should emphasize that, for the considered molecular ions, the yields recorded for triacontane spin-coated on metal substrates are quite similar for the two metals, Ag and Au (parts a and b of Figure 5). In contrast, results reported by Delcorte et al. for the molecular ion of Irganox 1010 indicate a 1 order of magnitude yield difference for the two metals.⁴¹ In our experiments, the most striking difference between Au and Ag occurs when they are used to metallize the triacontane layer. While the condensation of Au atoms on top of sample surface strongly increases the emission yields, the use of silver leads to an important yield decrease.

This comparison was extended in order to study the case of larger molecules such as metal-cationized ions emitted in the same conditions. The behavior is reminiscent of what was presented above for quasi-molecular ions. While $(\text{M} + \text{Au} - 2\text{H})^+$ ions have almost the same yield whether the molecule is spin-coated on a Au substrate or metallized by 10 nm Au, the heavier ions $(\text{M} + 2\text{Au} - \text{H})^+$ and $(\text{M} + 2\text{Au})^+$ are emitted with yields ~ 4 times higher when the molecule is spin-coated on the Au substrate (Figure 5c). Once again, the condition to obtain the highest yields for silver experiments is to spin-coat the triacontane on a Ag substrate instead of condensing Ag on

(49) Medvedeva, M.; Wojciechowski, I.; Garrison, B. J. *Appl. Surf. Sci.* **2003**, *203–204*, 148.

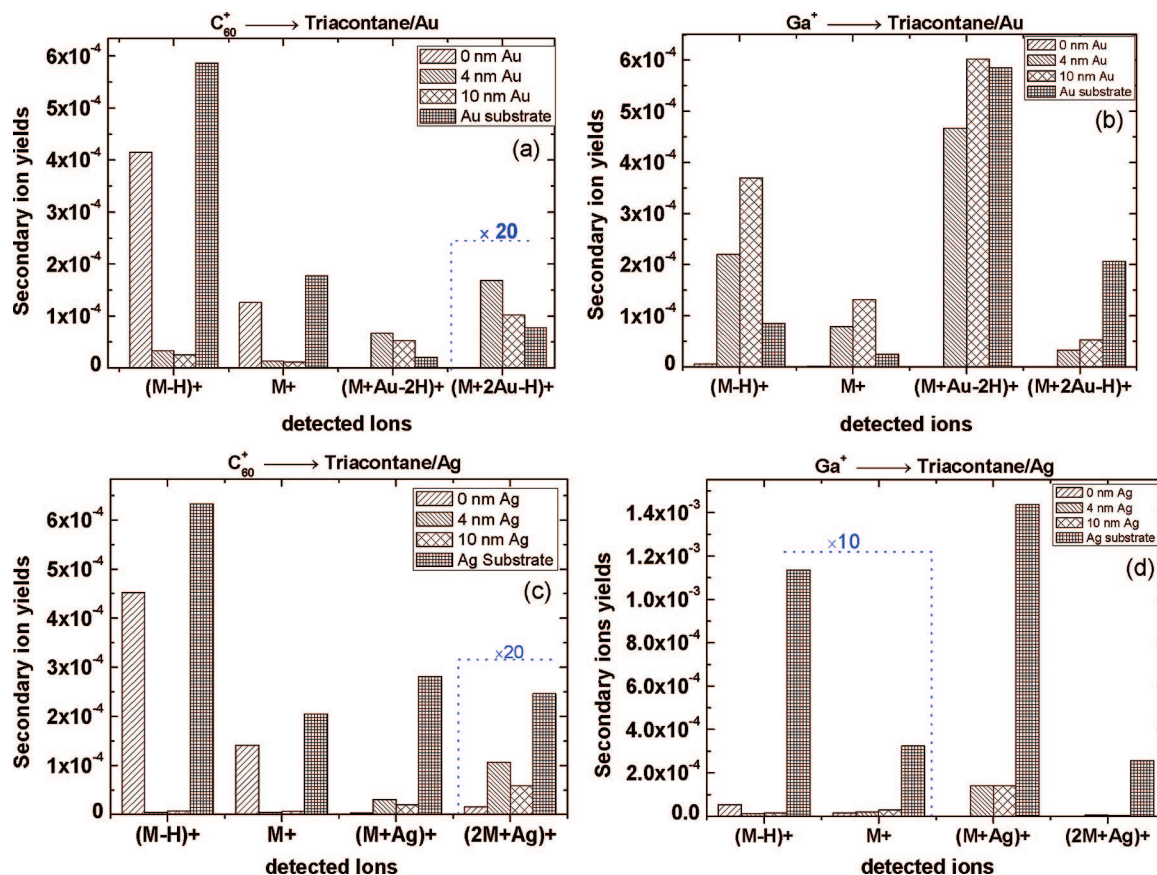


Figure 6. Secondary ion yields measured after gold and silver evaporation on triacontane layers and, on the other hand, the triacontane spin-coated on gold and silver substrates. In each frame the yields obtained for pristine sample (for molecular ions) as well as for two different Au/Ag thickness layers (4 and 10 nm) are depicted and compared with the results measured on the metal substrate. This comparison is made for several quasi-molecular ions as well as for metal-cationized ions under C_{60}^+ (a and c) and Ga^+ bombardment (b and d). Some histograms have been multiplied by 10 or 20 for a better visualization of the evolutions.

the molecular surface, whatever the thickness of the condensate. Between these two situations, the secondary ion yield ratio is huge. For example, the yield ratios for the $(M + Ag - xH)^+$ ions at $m/z = 527.4$ and 529.4 are close to 23 and 11, respectively (Figure 5d). The effect is even more pronounced in the case of $(M + 2Ag - xH)^+$ at $m/z = 637.4$, and $(2M + Ag - xH)^+$ at $m/z = 949.88$, for which the secondary ion yield ratios reach 80 and 77, respectively. Other studies using different organic molecules have also shown that metal substrates (Au and Ag) can give rise to secondary intensities up to a factor of 10 higher than the metallization method.³⁸

Gold and Silver Metallized Sample: Comparison between C_{60}^+ and Ga^+ Bombardment. The effects on the ion yields of triacontane spin-coated on Au and Ag substrates and the comparison with results obtained for Au and Ag metallized triacontane layers were also studied using polyatomic projectiles. The yields measured upon C_{60}^+ bombardment for the pristine and two metallized samples (4 and 10 nm) are presented in parts a and c of Figure 6 for several secondary ions (quasi-molecular and metal-cationized ions). They are compared to the yields measured for molecules spin-coated on Au (Ag) substrates. In the two others frames (Figure 6b,d), we show the corresponding results from Ga^+ experiments for a direct visual comparison. In the frames some ion yields are multiplied by a factor of 10 or 20 for a better visualization.

Part a ($Au-C_{60}^+$) shows two distinct situations. First, the yields of quasi-molecular ions $(M - H)^+$ and M^+ are higher when the molecule is spin-coated on a gold substrate. The yields measured for samples spin-coated on Si (pristine, 0 nm Au) and Au are 1 order of magnitude higher than those measured after evaporation of 4 or 10 nm Au on top of the samples. This is the first important difference with Ga^+ experiments for which the evaporation of 10 nm of Au on top of triacontane samples provided the highest yields for both molecular ions (Figure 6b). Second, for the Au-cationized ions $(M + Au - 2H)^+$ and $(M + 2Au - H)^+$, the yields are slightly higher, upon C_{60}^+ bombardment, after evaporation of 4 and 10 nm of Au than for spin-coating.

The measurements carried out using silver are presented in Figure 6c,d. Upon C_{60}^+ projectiles, the behavior of quasi-molecular ions $(M - H)^+$ and M^+ is very similar to that shown in the case of gold experiments. The yields are always higher when the molecule is spin-coated on Si (pristine) or Ag substrates rather than metallized by Ag layers whatever their thickness (Figure 6c). Once again, the highest yields are reached when using Ag as a substrate. The case of Ga^+ is similar at least for molecule spin-coated on Ag substrate, which provides the highest quasi-molecular ions yields (Figure 6d). The striking difference between C_{60}^+ and Ga^+ experiments concerns the large yield difference between samples spin coated on Ag and on Si (more than 1 order of magnitude), observed in the case of Ga^+ projectiles and not

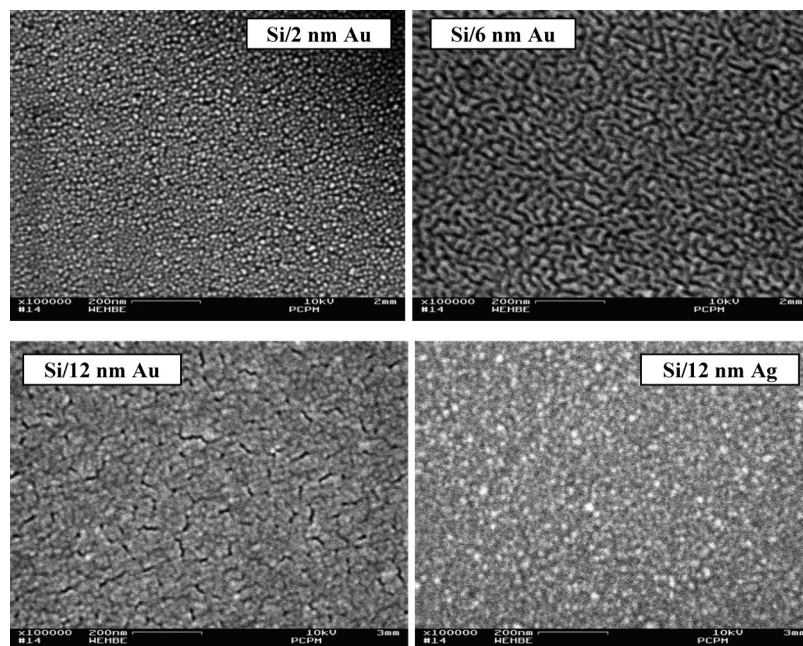


Figure 7. Scanning electron microscope (SEM) images showing the morphology of the Si wafer metallized with 2, 6, and 12 nm Au as well as with 12 nm Ag.

with fullerenes. As was the case for gallium measurements, the yields of $(M - H)^+$ and M^+ ions recorded under fullerene impact are comparable for samples spin-coated on Ag and Au substrates.

The behaviors of Ag-cationized ions, $(M + Ag - xH)^+$ and $(2M + Ag - xH)^+$, are similar for both C_{60}^+ and Ga^+ experiments (Figure 6c,d). Indeed, the highest yields are for molecules spin-coated on Ag substrates and not for Ag metallized samples. For instance, the ion yields for $m/z = 529.4$ are 10 times higher when triacontane is spin-coated on Ag substrate instead of metallized, whatever the thickness of the evaporated layer.

Mechanisms. Several arguments have already been proposed in order to explain the molecular ion yield enhancement effect of metallization in SIMS. The current interpretations generally involve the diffusion of organic molecules over the evaporated metal layer or the penetration of the metal particles through the organic material. Indeed, the morphology of the metallized samples, obtained using scanning electron microscopy (SEM), indicates that Au atoms coalesce to form dropletlike islands on the surface (see in Figure 7). These observations are supported by other studies, which investigated the growth of gold on polymers,⁵⁰ glass, and silicon substrates.^{51–53} Because of this structure, organic molecules can diffuse on the islands and mimic the situation of organic monolayers on gold substrates. In contrast with this interpretation, the enhancement of the triacontane ion yields even after the formation of a continuous gold layer (>15 nm) is difficult to understand because such a thick layer should block the emission and also the diffusion of buried organic molecules. To explain this result, one must assume that analyte diffusion and association with the gold and silver islands already

occur upon sputter-coating. Reports on the morphology and growth mechanisms of silver overlayers also exist in the literature. For benzene multilayers, Whitten et al.⁵⁴ showed that, after deposition of a few monolayers of silver, the Ag atoms penetrate deep into the benzene substrate and, instead of growing layer-by-layer, they form clusters beneath the surface. A similar behavior was described for silver and copper evaporated on polymer substrates.^{55–57} Although the growth of silver on silicon surfaces also involves an islandlike structure, our SEM analyses indicate that, for the same fluence, the silver islands are smaller than the gold islands as was already seen by Adriaensen et al.³⁸ (Figure 7). Concerning the metal coverage effect, it is useful to mention that another experimental study reports the detection of Ag-cationized ions even after evaporation of 22 nm of silver on top of the polymer surface.⁵⁸

The results in Figure 2 show that, while the quasi-molecular ion yields increase with the gold coverage only upon atomic projectile bombardment, they decrease strongly upon polyatomic projectiles compared to those measured for the pristine sample. In parallel, the Au-cationized molecular ion evolutions (Figure 3) upon polyatomic projectiles are similar but with comparatively lower yields than in the case of atomic projectiles. In the case of low mass monatomic primary ions (Ga^+ , In^+), the sputtering yields should increase with the gold deposition, because the gold islets, with a large stopping power, help to confine the Ga^+ and In^+ ion energy in the top surface layer. The adsorbed molecules are therefore more efficiently sputtered. In contrast, polyatomic

(50) Travaly, Y.; Zhang, L.; Zhao, R.; Uhrich, K.; Cosandey, F.; Garfunkel, E.; Madey, T. E. *J. Mater. Res.* **1999**, *14*, 3673–3683.
 (51) Semaltianos, N. G.; Wilson, E. G. *Thin Solid Films* **2000**, *366*, 111–116.
 (52) Doron-Mor, I.; Barkay, Z.; Filip-Granit, N.; Vaskevich, A.; Rubinstein, I. *Chem. Mater.* **2004**, *16*, 3476–3483.
 (53) Zymierska, D.; Auleytner, J.; Domagala, J.; Kobiela, T.; Dus, R. *Acta Phys. Pol., A* **2002**, *102*, 289–294.

(54) Whitten, J. E.; Gomer, R. *J. Phys. Chem.* **1996**, *100*, 2255–2259.
 (55) Pattabi, M.; Rao, K. M.; Sainkar, S. R.; Sastry, M. *Thin Solid Films* **1999**, *338*, 40–45.
 (56) Kundu, S.; Hazra, S.; Banerjee, S.; Sanyal, M. K.; Mandal, S. K.; Chaudhuri, S.; Pal, A. K. *J. Phys. D* **1998**, *31*, L73–L77.
 (57) Gollier, P.-A.; Bertrand, P. *Polymer-Solid Interfaces*. Proceedings of the Second International Conference, Namur, Belgium, Aug 12–16, 1996, p 173.
 (58) Ruch, D.; Muller, J. F.; Migeon, H. N.; Boes, C.; Zimmer, R. *J. Mass Spectrom.* **2003**, *38*, 50–57.

primary ions already deposit most of their energy in the upper organic layer of the pristine material, inducing very large emission yield. We have shown in Yield of Quasi-Molecular Ions that, upon Bi_3^+ , the yield of the molecular $(\text{M} - \text{H})^+$ and dimer $(2\text{M} - 2\text{H})^+$ ions for the pristine sample are, respectively, 2 and 3 orders of magnitude higher than those measured with the atomic Ga^+ primary ions. After gold condensation, the diffusion of a very thin molecular overlayer on top of the gold islets only limits the yield because of the small amount of organic material actually present on the surface. The results obtained with Bi_3^+ clusters allow us to generalize previous observations involving C_{60}^+ primary ions. It appears that the reduction of molecular ion yields upon metallization is not specific to fullerene projectiles but extends to other types of clusters. Qualitatively, these new results are in agreement with the interpretation already developed in ref 42 for C_{60} bombardment. Nonetheless, the very large extent of the observed yield variations also suggests the additional influence of ionization effects which might be specific to each projectile-sample combination. The presence of metal at the sample surface should play a major role in the ionization step of the emission process by locally changing the band structure and the work function of the surface.³⁵

The evolution of gold cluster intensities (Au_7^+ , Au_{13}^+ in Figure 4) can be tentatively explained on the basis of the specifics of the sputtering process, considering the different energy deposition depth of different primary ions. Because polyatomic ions such as C_{60}^+ already deposit their energy in the topmost layers of the surface, it is plausible that the emission yields of clusters decrease simply because their average binding energy to the surface increases with increasing metal coverage. In contrast, in order to observe high action events and large metal cluster emission under atomic ion bombardment, the energy of atomic projectiles must remain confined in the surface layer, which does not happen with organic substrates. In this context, it is reasonable to assume that increasing the thickness of metal will increase the probability of energy confinement and, thereby, the yield of clusters such as Au_7^+ and Au_{13}^+ up to a point where the binding energy effect offsets this increase. Our interpretation does not take into account possible electronic effects. Nevertheless, for gold clusters whose ionization state is mostly ruled by electronic exchange with the surface and do not involve more complex processes (proton exchange, rearrangements), the effect of the projectile nature on ionization should, in our opinion, not be prevalent.

Figure 5 shows that silver is beneficial only if it is used as a substrate rather than a condensate on top of the organic sample. This effect concerns both the metal-cationized species and the quasi-molecular ions. A large difference of behavior between organic monolayers cast on silver and silver metallized organic samples was reported in a previous study for Irganox samples.⁴¹ In that case, the M^+ and the $(\text{M} + \text{Ag})^+$ Irganox ions were emitted with yields, respectively, 237 and 67 times higher when Irganox was spin-coated on silver substrate rather than metallized by 2

nm of silver. In comparison, the quasi-molecular and metal-cationized ions were emitted with higher yields when Irganox was metallized by 2 nm of gold rather than spin-coated on gold substrates. The reasons of these differences remain unclear. It is possible that, after evaporation, silver atoms are deposited and associated with triacontane molecules to form a microstructure different than that formed using gold atoms (Figure 7).

CONCLUSION

The evolutions of the secondary ion yields as a function of the quantity of gold evaporated on triacontane samples are very dependent on the projectile nature (atomic or polyatomic). In the case of atomic bombardment (Ga^+ , In^+), quasi-molecular and Au-cationized ion yields increase with the gold fluence up to ~ 6 nm equivalent thickness, beyond which they remain almost constant in the investigated thickness range. As was previously reported for other types of samples, the yield enhancement factor between the gold metallized sample and the pristine sample can be large. For instance, with Ga^+ primary ions, the emission yield of the deprotonated molecular ion $(\text{M} - \text{H})^+$ is multiplied by a factor of ~ 70 after evaporation of 10 nm of Au. The enhancement of the triacontane ion yields even after the formation of a continuous gold layer (> 15 nm) is explained by assuming the diffusion of organic molecules over the evaporated metal layer or the penetration of the metal particles through the organic material already during the sputter-coating process. Contrary to the atomic projectile case, upon cluster projectile bombardment (Bi_3^+ , C_{60}^+), the presence of gold evaporated on the pristine samples leads to a drastic yield decrease for the quasi-molecular ions. The Au-cationized ions are always detected. Their yields were seen to increase up to 4 nm of Au. The basic difference between atomic and cluster primary ions is tentatively explained by arguments involving the different energy deposition mechanisms of these projectiles. Our results show clearly that the choice of metal plays a major role for the yield enhancement of the characteristic ions, e.g., Au and Ag do not induce the same behavior in MetA-SIMS. While spin-coating the triacontane molecules on a silver substrate provides always much higher yields than silver condensation on top of samples (whatever the amount of silver), experiments with gold show quite different results. The reasons of these differences may involve the different microstructures created upon condensation of gold and silver on the organic sample. More experiments are needed to clarify this point.

ACKNOWLEDGMENT

The European Community is acknowledge for funding N.W. and supporting this work through the Network of Excellence Nanobeams (Contract No. NMP4-CT-2004-500440).

Received for review March 19, 2008. Accepted June 10, 2008.

AC800568Y